0022-3565/07/3211-400–408$20.00
THE JOURNAL OF PHARMACOLOGY AND EXPERIMENTAL THERAPEUTICS
Vol. 321, No. 1
116202/3189465
Printed in U.S.A.

JPET 321:400–408, 2007

A Metabolic Screening Study of Trichostatin A (TSA) and TSA-Like Histone Deacetylase Inhibitors in Rat and Human Primary Hepatocyte Cultures

G. Elaut, G. Laus, E. Alexandre, L. Richert, P. Bachellier, D. Tourwé, V. Rogiers, and T. Vanhaecke

Departments of Toxicology (G.E., V.R., T.V.) and Organic Chemistry (G.L., D.T.), Vrije Universiteit Brussel, Brussels, Belgium; Laboratoire de Chirurgie Expérimentale, Fondation Transplantation, Strasbourg, France (E.A., L.R.); and Centre de Chirurgie Viscérale et de Transplantation, Hôpital de Hautepierre, Strasbourg, France (P.B.)

Received October 26, 2006; accepted January 10, 2007

ABSTRACT

Hydroxamic acid (HA)-based histone deacetylase (HDAC) inhibitors, with trichostatin A (TSA) as the reference compound, are potential antitumoral drugs and show promise in the creation of long-term primary cell cultures. However, their metabolic properties have barely been investigated. TSA is rapidly inactivated in rodents both in vitro and in vivo. We previously found that 5-(4-dimethylaminobenzoyl)aminovaleric acid hydroxyamide or 4-Me$_2$*N*-BAVAH (compound **1**) is metabolically more stable upon incubation with rat hepatocyte suspensions. In this study, we show that human hepatocytes also metabolize TSA more rapidly than compound **1** and that similar pathways are involved. Furthermore, structural analogs of compound **1** (compounds **2**-**9**) are reported to have the same favorable metabolic properties. Removal of the dimethylamino substituent of compound **1** creates a very stable but 50% less potent inhibitor. Chain lengthening (4 to 5 carbon spacer) slightly improves both potency and metabolic stability, favoring HA reduction to hydrolysis. On the other hand, Cα-unsaturation and spacer methylation not only reduce HDAC inhibition but also increase the rate of metabolic inactivation approximately 2-fold, mainly through HA reduction. However, in rat hepatocyte monolayer cultures, compound **1** is shown to be extensively metabolized by phase II conjugation. In conclusion, this study suggests that simple structural modifications of amide-linked TSA analogs can improve their phase I metabolic stability in both rat and human hepatocyte suspensions. Phase II glucuronidation, however, can compensate for their lower phase I metabolism in rat hepatocyte monolayers and could play a yet unidentified role in the determination of their in vivo clearance.

Histone deacetylase inhibitors (HDACi) have a high therapeutic potential as antitumoral drugs (Cohen et al., 1999; Piekarz and Bates, 2004; Vanhaecke et al., 2004b) and are being explored as new agents to prevent and/or treat several inflammatory diseases (Niki et al., 1999; Rombouts et al., 2002; Hockly et al., 2003; Rahmani et al., 2005; Blanchard et al., 2005a). In addition, they are components of a new strategy to prevent the spontaneous dedifferentiation of primary cells when isolated from their originating tissues and to positively affect the maturation of expanded stem cells. Exciting results have been obtained with respect to the long-term cultivation of primary rat hepatocytes and the creation of hepatocyte-like cells from adult rat and human bone marrow (Papeleu et al., 2003; Rogiers et al., 2004; Vanhaecke et al., 2004a; Snykers et al., 2006; Vinken et al., 2006).

Several structurally divergent classes of HDACi have now been synthesized or discovered. They are characterized by the size of their cap group and the nature of their functional group (Piekarz and Bates, 2004; Vanhaecke et al., 2004b). Hydroxamic acid (HA)-based small molecule HDACi, structurally derived from the naturally occurring compound (*R*)-(+)-trichostatin A (TSA, Table 1), constitute one of the most important classes because they potently inhibit HDAC in a reversible way (Finnin et al., 1999). One of these TSA analogs, SAHA (suberoylanilide hydroxamic acid, vorinostat), is

This work was supported by grants from the Fund for Scientific Research-Flanders (FWO) and the Research Council (OZR) of the Vrije Universiteit Brussel (Brussels, Belgium). This work is also part of the European Specific Targeted Research Project-Project Predictomics 504761.

Article, publication date, and citation information can be found at http://jpet.aspetjournals.org.

doi:10.1124/jpet.106.116202.

ABBREVIATIONS: FBS, fetal bovine serum; HA, hydroxamic acid; HDAC, histone deacetylase; HDACi, histone deacetylase inhibitor(s); HPLC, high-performance (pressure) liquid chromatography; LDH, lactate dehydrogenase; 4-Me$_2$*N*-BAVAH, 5-(4-dimethylaminobenzoyl)aminovaleric acid hydroxyamide; QSAR, quantitative structure-activity relationship; SAHA, suberoylanilide hydroxamic acid; TSA, *R*-(+)-trichostatin A or 7-[4-(dimethylamino)phenyl]-4,6-dimethyl-7-oxo-hepta-2,4-dienoic acid hydroxamide; DMSO, dimethyl sulfoxide.

TABLE 1

Chemical structures, in vitro rat hepatocyte HDAC inhibition data, and major phase I biotransformation pathways of TSA and the synthesized amide-linked analogs in rat hepatocyte suspensions

Benzamides **1** to **7** were prepared as described previously by Jung et al. (1997, 1999); compounds **8** and **9** were synthesized as described by Van Ommeslaeghe et al. (2003). HDAC inhibition determinations and biotransformation experiments were performed as described under *Materials and Methods*.

Compound	Chemical Structures	IC_{50} Rat Liver HDAC	Major Phase I Biotransformation Pathway	Major Phase I Metabolite(s) after 3 h of Incubation
		nM		
TSA	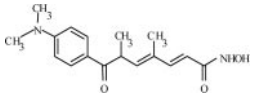	11 ± 2	*N*-Demethylation, HA reduction	*N*-Didemethylated amide
1	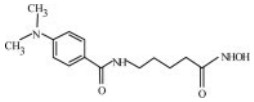	1920 ± 405	HA hydrolysis, HA reduction	Carboxylic acid, amide
2	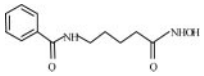	4218 ± 681	HA hydrolysis	Carboxylic acid
3	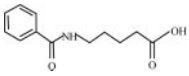	$>10^6$		
4	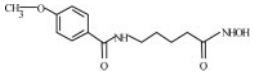	3109 ± 294	HA hydrolysis	Carboxylic acid
5	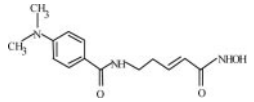	3978 ± 614	HA reduction	Amide
6	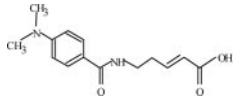	$>10^6$		
7	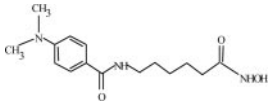	152 ± 15	HA reduction	Amide
8	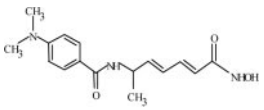	12,187 ± 1384		
9	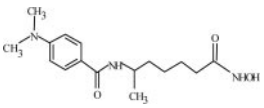	359 ± 92	HA reduction	Amide

currently in phase I and II clinical trials for the treatment of hematologic and solid tumors (Kelly and Marks, 2005; Krug et al., 2006).

Xenobiotic biotransformation is generally recognized as a key determinant of the efficacy and toxicity of a potential new drug (Li, 2001; Elaut et al., 2002). However, little information on the biotransformation of HA-based HDACi is available in the current literature, and attempts to optimize their metabolic properties have been scarce. We previously showed that 50 μM TSA is completely inactivated within 40 min upon incubation with rat hepatocyte suspensions (Elaut et al., 2002). Another group (Sanderson et al., 2004) subsequently reported a half-life of 6.3 min upon peritoneal administration of TSA (0.5 mg · kg) to mice. Likewise, SAHA displays a low half-life (2–3 min) in rat (Cohen et al., 1999).

In the search for metabolically more stable TSA derivatives, we recently found the amide-linked analog 5-(4-dimethylaminobenzoyl)aminovaleric acid hydroxyamide or 4-Me_2*N*-BAVAH [further referred to as compound **1** (Table 1)] to be considerably more resistant to metabolic inactivation by rat hepatocytes in suspension (Elaut et al., 2004). This could imply that simple structural modifications of the TSA aliphatic spacer already can generate significantly more stable inhibitors.

We now report data on the biotransformation of eight other amide-linked TSA analogs (compounds **2**-**9**) (Jung et al., 1997, 1999; Van Ommeslaeghe et al., 2003) (Table 1) in rat hepatocyte suspensions. Furthermore, because no human data are available yet in the current literature, the metabolic properties of TSA, compound **1** and the most stable and active analog **7**, are studied in human hepatocyte suspensions. Finally, because of the potential use of TSA-like HDACi to optimize primary hepatocyte cultures, a series of experiments is performed with rat hepatocyte monolayers. This also gives us the opportunity to identify potential phase II biotransformation pathways and elucidate the metabolic patterns after long-term exposure.

Materials and Methods

Chemicals and Reagents. Acetonitrile (HPLC grade), β-glucuronidase from bovine liver B-3, β-glucuronidase-sulfatase mollusk

H-1, bovine insulin, bovine serum albumin fraction, crude collagenase type I, HEPES, kanamycin monosulfate, L-glutamine, $MgCl_2$, TSA or 7-[4-(dimethylamino)phenyl]-4,6-dimethyl-7-oxo-hepta-2,4-dienoic acid hydroxamide (purity ≥98%), trypan blue, sodium ampicillin, streptomycin sulfate, and sucrose were purchased from Sigma-Aldrich (Bornem, Belgium). Hydrocortisone sodium hemisuccinate came from Pharmacia (Brussels, Belgium), Williams' E medium was from Invitrogen (Brussels, Belgium), and fetal bovine serum (FBS) was from Invitrogen. Heparin and glucagon were obtained from Novo Nordisk (Copenhagen, Denmark). Trifluoroacetic acid of analytical reagent grade, sodium acetate, Tris·HCl, KCl, and ethyl acetate were from VWR International (Leuven, Belgium). Insta-gel plus scintillation cocktail came from Packard Bioscience B.V. (Groningen, The Netherlands).

Synthesis of the Amide-Linked Analogs. Benzamides **1-7** (Table 1) were prepared as described previously by Jung et al. (1997, 1999) by coupling of the benzoic acid to the methyl ester of 5-aminovaleric acid, 6-aminohexanoic acid, and (*E*)-5-amino-2-pentenoic acid, followed by saponification of the ester, formation of the *O*-benzyl hydroxamate, and hydrogenolysis. Compounds **8** and **9** (Table 1) were synthesized as described by Van Ommeslaeghe et al. (2003). The *O*-benzyl group of compounds **5** and **8** was removed by treatment with liquid anhydrous hydrogen fluoride. Stock solutions (200 mM) of each compound and of TSA were prepared in DMSO, stored at −20°C, and diluted as required for each experiment.

Determination of in Vitro HDAC Inhibition Potency. The inhibition of HDAC activity in crude rat hepatocyte lysates was assessed according to the procedure described by Kölle et al. (1998), with some modifications. Freshly isolated rat hepatocytes (see next paragraph) were homogenized by sonication (Labsonic U; B. Braun Laboservice N.V., Kontich, Belgium) in a 50 mM Tris·HCl buffer, pH 7.5, containing 0.25 mM sucrose, 25 mM KCl, and 5 mM $MgCl_2$. Protein concentrations, after centrifugation (10000*g*, 5 min, 4°C), were determined according to the Bradford procedure (Bradford, 1976) using a Bio-Rad protein assay kit (Bio-Rad, Brussels, Belgium), with bovine serum albumin as a standard. Enzyme preparation aliquots of 25 μl (protein concentration, 6 mg/ml) were mixed with 5 μl of compound solution and preincubated on ice for 15 min. The reaction (30°C, 20 min) was started by the addition of 10 μl of [^{3}H]acetate-prelabeled histones (1 mg/ml) and terminated with 36 μl of 1 M HCl/0.4 M sodium acetate and 800 μl of ethyl acetate. After centrifugation (10000*g*, 5 min), [^{3}H]acetate in the upper ethyl acetate phase was estimated by radioactive counting. For determination of the 50% inhibitory concentrations (IC_{50}), six concentrations of each compound (within the range of 5 nM-100 μM) were tested in triplicate. Homogenization buffer and 0.05% v/v DMSO were used as negative controls, whereas incubations with a 5-min boiled cell extract served as a blank.

Incubations with Primary Rat Hepatocytes. A two-step collagenase perfusion technique (Papeleu et al., 2006) was used to isolate the hepatocytes from the liver of male outbred Sprague-Dawley rats (200–300 g; Charles River Laboratories, Brussels, Belgium), which were kept under controlled environmental conditions (12-h light/dark cycle) and fed a standard diet (Animalabo A 04) with water ad libitum. Procedures for the accomodation of the animals and for the isolation and cultivation of the rat hepatocytes were approved by the local ethical committee of the Vrije Universiteit Brussel (Brussels, Belgium).

Freshly isolated hepatocyte suspensions (2×10^6 cells/ml, HEPES buffer, pH 7.65, 37°C) were exposed to TSA, the synthesized HA-containing analogs, or the solvent control (0.1% v/v DMSO) for 3 h. Samples for biotransformation (extracellular medium) and lactate dehydrogenase (LDH) index analyses were taken (Elaut et al., 2002, 2005). Nonmetabolic degradation was assessed by incubation with 2-min boiled cells.

To investigate long-term biotransformation and in particular potential phase II conjugation of TSA and compound **1**, rat hepatocyte monolayer cultures were used. Freshly isolated rat hepatocytes were cultured on 35-mm (φ) Petri dishes at a density of 1.12×10^5 cells/cm^2 at 37°C in an atmosphere of 5% CO_2 and 95% air and 100% relative humidity. After plating in Williams' E medium supplemented with 10% v/v FBS, 2 mM L-glutamine and antibiotics (7.3 IU/ml benzylpenicillin, 50 μg/ml streptomycin sulfate, 50 μg/ml kanamycin monosulfate, and 10 μg/ml sodium ampicillin), the cells were allowed to attach to the plastic substrate for 4 h. Serum-containing medium then was removed, and fresh serum-free culture medium supplemented with hydrocortisone sodium hemisuccinate (0.5 μg/ml), glucagon (0.007 μg/ml), and bovine insulin (5 μg/ml) was added. One-day-old cultures were exposed to TSA (25 μM), compound **1** (50 μM), or the solvent control (0.05% v/v DMSO) during 24 h. Medium samples for biotransformation analysis were taken by submersion of 1-ml aliquots in liquid nitrogen. For studying the intracellular biotransformation profiles, the cell monolayer was scraped off and washed in ice-cold phosphate-buffered saline. The collected cell pellets were sonicated (Labsonic U; B. Braun Laboservice N.V.) in methanol (1 ml) and centrifuged (2000*g*, 30 min, 4°C), and the supernatants were stored at −80°C until further analysis.

Incubations with Primary Human Hepatocytes. Adult normal liver samples were obtained from 16 patients (male/female, aged 22–68) undergoing partial hepatectomy for primary or secondary liver tumors. The hepatocytes were isolated by a two-step collagenase perfusion through the existing vasculature or by direct injection of collagenase into the liver parenchyma (Alexandre et al., 2002). All experimental procedures were done in compliance with French laws and regulations and were approved by the National Ethics Committee. After Percoll purification (33% v/v) (Chesné et al., 1993), cell viability was estimated by trypan blue dye exclusion (45–86%). The freshly isolated cells in suspension were either used directly for incubation (three donors) or cryopreserved for later use by the progressive freezing procedure described previously by Alexandre et al. (2002) (12 donors). To be able to analyze differences induced by the cryopreservation procedure, cells isolated from the 16th patient were partly used directly and partly cryopreserved for later biotransformation experiments.

Incubations were carried out with either 50 μM TSA, 50 μM compound **1**, 0.025% v/v DMSO, or only buffer in conditions identical to the ones used for rat (Elaut et al., 2004). Cryopreserved cells (stored for no longer than 6 years) were thawed by immersion in a 37°C water bath. DMSO was removed by dilution with Leibovitz L-15 medium containing 10% v/v FBS, and the hepatocytes were washed and suspended in HEPES buffer (pH 7.65, 4°C). Cell number, viability, and yield were assessed by trypan blue dye exclusion. Percoll (20% v/v) purification of the thawed hepatocytes was only performed when cell viability was low (< 60%).

Determination of Cell Membrane Damage. Hepatocyte membrane damage was evaluated by determination of the LDH index (= 100 × LDH activity in the supernatant divided by the sum of LDH activity in the supernatant and in the cells) using a Merckotest (VWR International, Leuven, Belgium).

Analysis of Biotransformation. Samples taken for determination of the intracellular amounts of parent compounds and metabolites were analyzed directly after thawing without further treatment. Samples for extracellular medium profile determinations were centrifuged (120*g*, 2 min, 4°C), and their supernatants were cleaned up by solid-phase extraction (Waters Oasis HLB Cartridges; Waters Corporation, MA) as described previously (Elaut et al., 2002, 2004). Information on reversible protein binding of the metabolites was obtained through treatment of the extracellular medium samples with an equal volume of acetonitrile:methanol (1:1), followed by centrifugation (200*g*, 30 min, 4°C). After drying (N_2, 45°C) and dissolving the samples in 60 mM sodium acetate/acetic acid buffer containing 0.11 M NaCl, they were extracted in a way similar to nontreated extracellular supernatants.

Separation of the mother compounds and their metabolites was performed by reversed-phase HPLC on a Discovery C18 (5 μm, 250 × 4.6 mm, Supelco; Sigma-Aldrich) or Alltima HP C18 column (5 μm,

250 × 4.6 mm; Alttech Associates Inc., Lokeren, Belgium) using a Gilson chromatographic system (Gilson International B.V. Rijswijk, The Netherlands), according to the method described previously (Elaut et al., 2002, 2004), albeit with small variations of the mobile phase gradient. UV detection was performed at 266 (TSA) and 255 nm (amide-linked structural analogs). For identification of the metabolites, the eluate was split (Acurate; LC Packings, Amsterdam, The Netherlands) to direct 10% to a VG Quattro II triple mass spectrometer with electrospray ionization interface applied in the positive mode with a mass range from *m/z* 110 to 850 (Micromass, Manchester, UK). Further structural identification was performed by tandem mass spectrometry fragmentation, with detection over a mass range of *m/z* 75 to 350 (Elaut et al., 2002).

To determine free and conjugated parent compounds and phase I metabolites, 500 μl of supernatant fractions were incubated (37°C, 12 h) with 700 μl of 60 mM acetate/0.11 M NaCl buffer supplemented with 10 mM saccharonolactone, 540 IU/ml β-glucuronidase-sulfatase H1, or 580 IU/ml β-glucuronidase B3. The relative abundances of the glucuronide and sulfate conjugates was determined semiquantitatively by comparing HPLC-UV peak areas before and after hydrolysis.

Statistical Analysis. Unless specified, the results are expressed as the mean (± S.D.) of at least three independent experiments. The group means were compared by a paired Student's *t* test (metabolic degradation, LDH index in rat hepatocyte cultures), an unpaired Student's *t* test (metabolic degradation rat/human, humans interindividually), or a two-way analysis of variance followed by a Student-Newman-Keuls test (metabolite formation). A $p < 0.05$ was considered to be statistically significant.

Results

Biotransformation of TSA and Compound 1 in Freshly Isolated and Cryopreserved Human Hepatocyte Suspensions. Suspensions of freshly isolated and thawed cryopreserved human hepatocytes were exposed to TSA and compound **1** under conditions similar to those described previously for rat hepatocytes (Elaut et al., 2004). In preliminary experiments, the LDH indices of the hepatocytes exposed to 50 μM of each compound within 3 h were evaluated. No increases in LDH index were observed in thawed cryopreserved or freshly isolated cells compared with control suspensions in buffer (results not shown).

The metabolic degradation of TSA by a suspension of thawed cryopreserved human hepatocytes pooled from five different donors (Fig. 1A) was slower compared with the rat hepatocyte suspensions. The latter fully degraded TSA within the 1st hour of incubation (Elaut et al., 2002). This was not due to the cryopreservation procedure, because no differences in the time-dependent breakdown of TSA between freshly isolated and thawed cryopreserved human hepatocytes, prepared from a same donor, were observed (Fig. 1B). Similar to rat hepatocytes (Elaut et al., 2002), human cells preferentially reduced and *N*-dealkylated TSA, resulting in the formation of TSA amide, and *N*-mono- and *N*-didemethylated TSA or TSA amide metabolites. There were no large differences in the nature of the major phase I metabolites produced in suspensions of thawed cryopreserved and freshly isolated human hepatocytes after 2 h of incubation (Table 2).

As observed in rat hepatocyte suspensions, the metabolic stability of compound **1** in a pool of thawed cryopreserved human hepatocytes was significantly higher than observed for TSA (Fig. 1A). Although the corresponding amide was a major metabolite of TSA, compound **1** preferentially underwent hydrolysis to produce the carboxylic acid (Table 2). *N*-Monodemethyl and carboxylic acid metabolites constituted approximately half of the total amount of metabolites produced after 2 h of incubation of compound **1** with cryopreserved human hepatocytes. A slightly more extensive *N*-demethylation of compound **1** was observed in freshly isolated cells, which resulted in the additional formation of small amounts of *N*-didemethylated **1** (Table 2).

For both TSA and compound **1**, no significant amounts of phase II metabolites could be detected upon treatment of the samples with β-glucuronidase H3/B1. Dinor dihydro acid me-

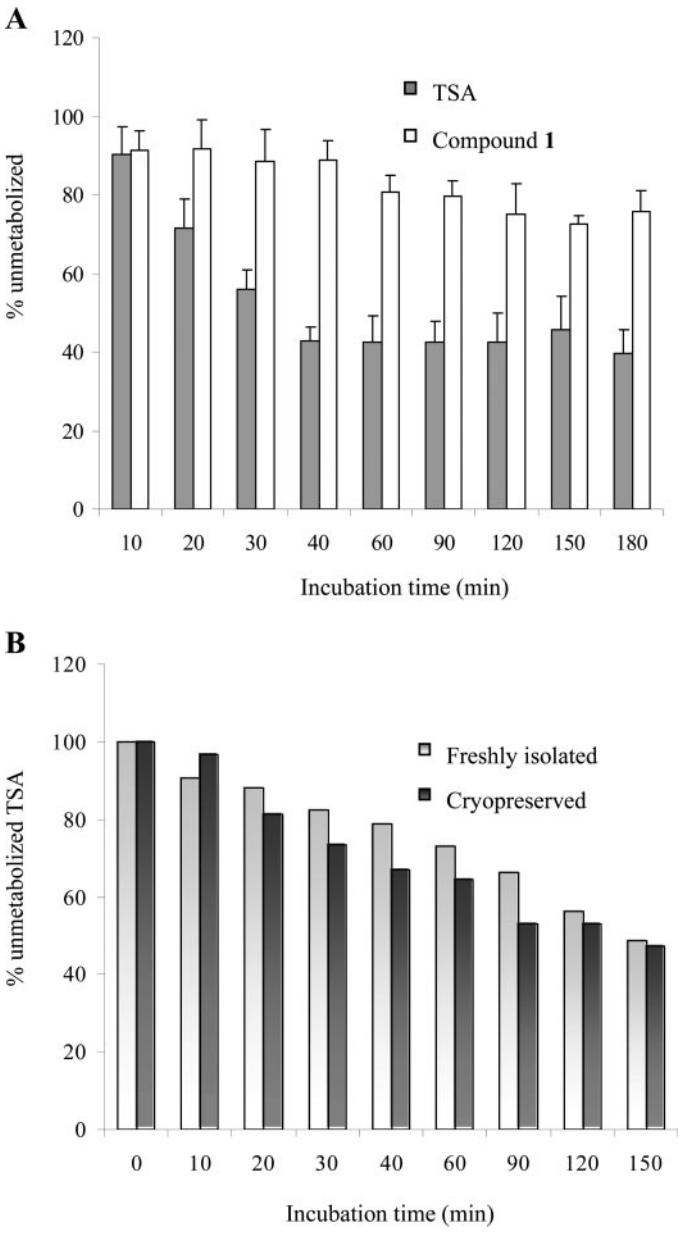

Fig. 1. A and B, metabolic degradation of 50 μM TSA and compound **1** in a pool of five cryopreserved hepatocyte suspensions (2×10^6/ml; viability 61.8%) as a function of the incubation time (A) and comparison of the metabolic degradation of 50 μM TSA in fresh and cryopreserved human hepatocytes obtained from the same donor (B). Parent compound concentrations in the extracellular medium were followed by HPLC-UV (at 266 and 255 nm for TSA and compound **1**, respectively). Results are expressed as percentage of unmetabolized compound (percentage of the peak area in samples taken immediately after addition of the compound stock solutions) ($n = 3$).

TABLE 2

Comparison of the relative abundances of the major phase I metabolites of TSA and compound **1** upon their incubation with suspension and cryopreserved and freshly isolated human hepatocytes within 2 h

The experiments were performed as described under Materials and Methods. For TSA, hepatocytes from a single donor were used. In the case of compound **1**, the indicated values are the average of results obtained with cryopreserved cells from 10 donors and with three different freshly isolated human hepatocyte incubations. For both inhibitors, a 50 μ M starting concentration was used. Peak areas obtained after HPLC-UV analysis of the samples were used to determine the relative abundances, e.g., the amount of each metabolite relative to the total amount of metabolite + parent compound (%).

Metabolite		Cryopreserved Hepatocytes	Freshly Isolated Hepatocytes
		%	
TSA	TSA amide	20	22
	Trichostatic acid	3	2
	N-Monodemethylated TSA	4	5
	N-Monodemethylated TSA amide	2	0
	N-Didemethylated TSA	6	10
	N-Didemethylated TSA amide	3	4
Compound **1**	**1**-Amide	2	6
	1-Acid	**7**	9
	N-Monomethylated **1**	6	2
	N-Didemethylated **1**	0	2
	N-Monodemethylated **1**-acid	4	9

tabolites could only be identified by tandem mass spectrometry upon manifold concentration of the samples (under N_2, 45°C).

Effect of Structural Modifications of Compound 1 on HDAC Inhibition Potency and Biotransformation Properties in Freshly Isolated Rat Hepatocyte Suspensions. As shown in Table 1, the synthesized analogs are structurally characterized by the linkage of an aromatic benzoyl nucleus to an aliphatic side chain through an amide bond. Whereas the *p*-substituent on the benzoyl fragment differs for compounds **1**, **2**, and **4** (-N(CH_3)$_2$, -H, and -OCH_3, respectively), analog **5** has an unsaturated (Cα) aliphatic chain. Compounds **1** to **6** share an aliphatic chain of four methylene groups, whereas compounds **7** to **9** possess a 5-carbon chain. With the exception of carboxylic acids **3** and **6**, which are potential phase I metabolites of compounds **2** and **5**, respectively (Elaut et al., 2002, 2004), the compounds contain a HA functional group. Because of the presence of a methyl substituent adjacent to the benzoyl fragment on their 5-carbon side chains, compounds **8** and **9** are structurally more similar to TSA.

Inhibition of Rat Hepatocyte HDAC. Table 1 shows that the synthesized amide-linked compounds are 10- to 1000-fold less potent in inhibiting rat HDAC than the reference compound TSA (IC_{50} = 11 nM). Similar to the results obtained by Jung et al. (1999) in maize HD-2, compound **7** (152 nM) is one order of magnitude more potent than **1** (1920 nM), demonstrating the importance of the spacer length (5-carbon versus 4-carbon spacer, respectively). The newly synthesized compound **1** derivatives, characterized by a removed *p*-dimethylamino substituent (compound **2**) and unsaturated aliphatic chain (compound **5**), display a 50% reduced enzyme inhibitory activity. Although derivatives **8** and **9** bear greater structural resemblance to TSA due to the presence of an aliphatic methyl substituent, their inhibiting powers are lower than compound **7**. The HDAC inhibitory activity drops with two orders of magnitude in the case of the diene **8**. Because of its low activity, this compound was not considered for biotransformation studies. As expected from other structure-activity data (Massa et al., 2001; Mai et al., 2003) and the HDAC inhibition mechanism (Finnin et al., 1999), the acid metabolites **3** and **6** do not significantly inhibit rat hepatocyte HDAC in the concentration range tested. However, they may constitute important phase I metabolites of compounds **2** and **5**, respectively (Elaut et al., 2004). Therefore, we screened their necrotic effects in freshly isolated rat hepatocyte suspensions and used their major metabolites to identify secondary metabolites of their HA-containing parent compounds.

Phase I Biotransformation in Freshly Isolated Rat Hepatocyte Suspensions. No acute necrotic effects (i.e., increases in LDH index) were observed during a 3-h exposure of freshly isolated rat hepatocytes to a 100 μM concentration of HA-containing analogs **2**, **4**, **5**, **7**, **8** and **9**. Likewise, no cytotoxicity was observed upon exposure of the hepatocytes to 25 μM of the acid compound **3**. However, 25 μM of the acid metabolite **6** of compound **5** significantly decreased hepatocyte viability (results not shown).

The metabolic breakdown of HA-containing amide-linked compounds **1, 2, 4, 5, 7,** and **9** (50 μM) in isolated rat hepatocyte suspensions is depicted in Fig. 2. Their major phase I biotransformation pathways identified are summarized in Table 1. *p*-Methoxy substitution of the benzoyl fragment (compound **4**) accelerated metabolic degradation compared

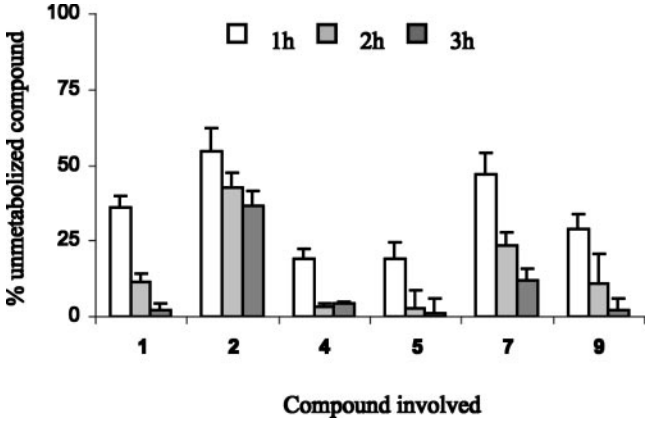

Fig. 2. Metabolic stabilities of the HA-containing TSA analogs **1**, **2**, **4**, **5**, **7**, and **9** in suspensions of freshly isolated rat hepatocytes. Two million hepatocytes per milliliter were exposed to 50 μM TSA or HA-based analog within 3 h. Parent compound concentrations in the extracellular medium were followed by HPLC-UV (at 266 and 255 nm for TSA and the analogs, respectively). Results are expressed as percentage of unmetabolized compound (percentage of the peak area in samples taken immediately after addition of the compound stock solutions) (n = 3) as a function of the incubation time.

with *p*-dimethylamino derivative **1**. This was not due to a lower inherent stability of the methoxy substituent, because only minor amounts of *O*-demethylated metabolites were found after 3 h of incubation. Unsubstituted compound **2** was more stable (37% compound **2** still present after 3 h). Whereas unsaturation of the aliphatic linker of compound **1** resulted in a more rapid degradation, lengthening to five methylene groups increased metabolic stability (compound **7**). This effect was abolished by methylation (compound **9**) of the aliphatic chain. The HA-moieties of compounds with a 5-C spacer were preferentially reduced, although the analogs with a shorter spacer were more readily hydrolyzed to carboxylic acids. The introduction of a double bond at the Cα position of compound **5** seemed to favor HA reduction.

Biotransformation of Compound 7 in Human Hepatocyte Suspensions. Because of its potent inhibitory capacity toward rat HDAC and its good metabolic stability in the presence of freshly isolated rat hepatocytes in suspension, compound **7** was selected for further incubations with a pool of five thawed cryopreserved human hepatocyte suspensions. The measured LDH indices showed that 50 μM was a suitable testing concentration (results not shown). As also observed in rat hepatocyte suspensions, compound **7** was found to be slightly more stable than compound **1**. It preferably underwent HA reduction and oxidative *N*-dealkylation (Fig. 3).

Biotransformation of TSA and Compound 1 in Monolayer Cultures of Freshly Isolated Rat Hepatocytes. As 50 μM TSA induced an increase in LDH index after a 24-h incubation with rat hepatocyte monolayer cultures, its concentration was reduced to 25 μM. No significant differences were observed when the monolayers were exposed for 24 h to 50 μM compound **1** or the control solvent (0.05 v/v% DMSO).

Figure 4, A and B, shows the time-dependent breakdown of TSA and compound **1** and formation of their major phase I and phase II metabolites, respectively, in the extracellular medium of 1-day-old adult rat hepatocyte monolayer cultures. Consistent with the results obtained in rat and human hepatocyte suspensions, TSA was readily *N*-demethylated. As a result, *N*-didemethylated TSA was the major metabolite in the extracellular medium during the first 2 h of incubation. Furthermore, because of the onset of a rapid HA-reduction process, *N*-didemethylated TSA, TSA amide, and *N*-didemethylated TSA amide were among the major phase I metabolites detected in 6-h samples. Monolayer cultures of

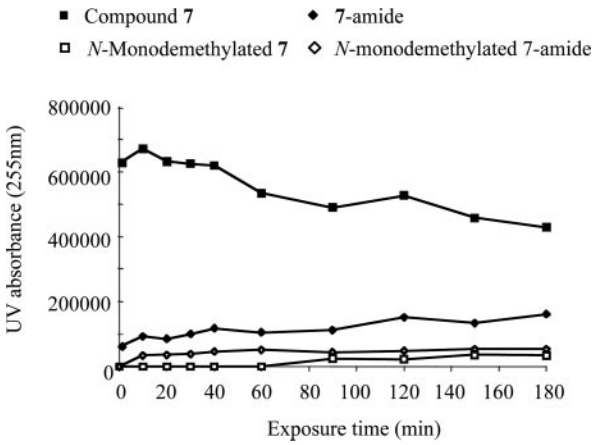

Fig. 3. Kinetics of compound **7** consumption and metabolite production in suspensions of cryopreserved human hepatocytes (pool of cells obtained from five patients). Two million hepatocytes per milliliter were exposed to 50 μM compound **7** for 3 h. The peak areas detected at 255 nm are shown as a function of the incubation time (n = 2).

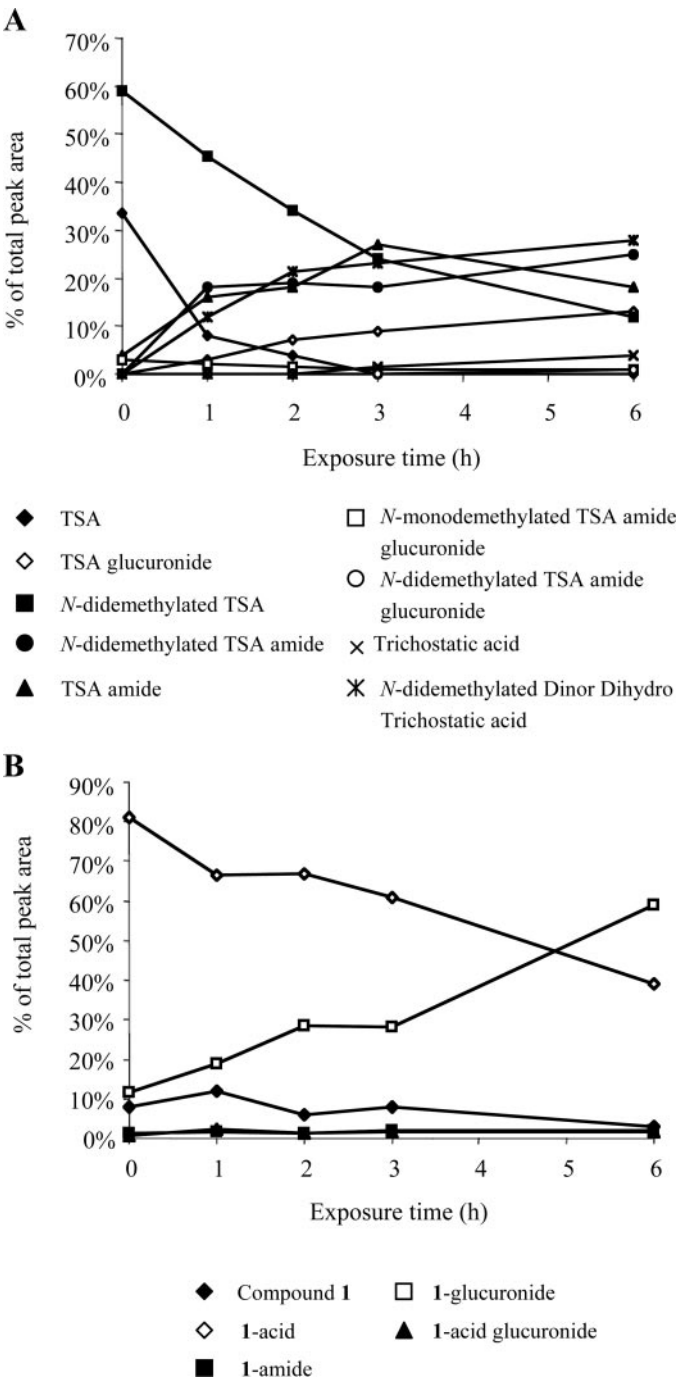

Fig. 4. A and B, phase I and phase II biotransformation of TSA (A) and compound **1** (B) in rat hepatocyte monolayer cultures. One-day-old hepatocytes were exposed to 25 μM TSA and 50 μM compound **1**, and samples were taken immediately after the addition of the medium containing the inhibitors (0 min) and after 1, 2, 3, and 6 h of exposure. Parent compound and metabolite concentrations in the extracellular medium were followed by HPLC-UV (TSA, 266 nm; compound **1**, 255 nm). Results (n = 3) are expressed as percentage of the total peak area in the samples taken at the indicated time points; means ± S.D. were omitted for clarity reasons. Because the extinction coefficients of the metabolites at the detection wavelength are not known, the results are semiquantitative. The amounts of glucuronide metabolites were derived from the differences in peak areas between nonhydrolyzed and β-glucuronidase B3-treated samples as described under *Materials and Methods*.

rat hepatocytes also formed relatively large amounts of *N*-monodemethylated dinor dihydro trichostatic acid (approximately 25% of the total amount of metabolites starting from 1 h of incubation), a metabolite produced in small amounts upon in vivo administration of TSA to mice (Sanderson et al., 2004) but not detectable in hepatocyte suspensions. Trichostatic acid, *N*-monodemethylated trichostatic acid, and dihydro trichostatic acid were minor metabolites. Whereas no phase II conjugations of TSA nor those of its phase I metabolites could be observed previously in hepatocyte suspensions (Elaut et al., 2002), a gradual glucuronidation of TSA, its *N*-demethylated amide metabolites, and trichostatic acid was seen in the monolayer cultures. TSA glucuronide, *N*-monodemethylated dinor dihydro trichostatic acid, and *N*-didemethylated TSA amide were among the major metabolites after 24 h of exposure (Table 3). The site of glucuronidation is currently unknown as a comparison of peak areas before and after hydrolysis was used here to determine the amount of phase II conjugates. No intracellular accumulation of the parent compound or its metabolites could be detected. However, upon protein precipitation before clean-up by solid-phase extraction, a 1.5-fold increase in total peak area was obtained. Comparison of the individual metabolite peak areas before and after protein precipitation revealed that *N*-didemethylated TSA amide glucuronide, trichostatic acid glucuronide, and dihydro dinor trichostatic acid were extensively bound to cellular and/or excreted proteins (Table 3).

Whereas TSA was more susceptible to phase I biotransformation than glucuronidation, a large amount (80%) of compound **1** was glucuronidated immediately upon exposure to the hepatocyte monolayers (Fig. 4B). As observed in suspensions, the monolayers initially did not *N*-demethylate compound **1** but preferentially formed the corresponding acid metabolite. Glucuronidated **1** and **1**-acid glucuronide were the major metabolites during the first 6 h of exposure (Fig. 4B). During the following hours, *N*-demethylation of both the parent compound and the **1**-acid metabolite resulted in the production of *N*-monodemethylated **1**-acid, *N*-monodemethylated **1**-acid glucuronide, and *N*-monodemethylated **1** as major metabolites after 24 h. In addition, considerable amounts of the reduced metabolite, **1**-amide, were formed (Table 3). Protein precipitation of the 24-h samples revealed that the sulfate conjugates of compound **1**, **1**-amide, and *N*-monodemethylated **1**-acid had a high protein affinity (Table 3).

Discussion

Among the different classes of HDACi now available, TSA and its structural analogs remain among the most interesting because of their potent and reversible inhibitory properties, as well as their relatively easy synthesis (Vanhaecke et al., 2004b; Elaut et al., 2006). However, they are metabolically unstable (Cohen et al., 1999; Elaut et al., 2004; Sanderson et al., 2004). Thus, it seems interesting to look for possibilities to improve their biotransformation properties. This will aid in the identification of the most appropriate compounds for further drug development and/or for the prevention of dedifferentiation of primary cells in culture.

In this study, we compared the rat hepatocyte HDAC inhibition potencies and in vitro biotransformation properties of nine structural amide-linked analogs of TSA (Table 1) in rat and man. We found that, although they are less potent inhibitors than TSA, all analogs are more resistant to phase I-dependent metabolic inactivation in both rat and human hepatocyte suspensions. Compounds **1**, **2**, and **7** were found to display the best balance between inhibition potency and metabolic stability. Importantly, structural modifications of the aliphatic spacer seem to affect both the rate and pathway of metabolic inactivation of the functional group.

Some observations recently made by our research team in primary hepatocyte cultures support the significance of a higher metabolic stability with respect to cellular efficacy. Although the IC_{50} values of TSA and compound **1** in rat hepatocyte lysates differ almost 200-fold (Table 1), only 50-

TABLE 3

Relative abundances of the phase I and II metabolites of TSA and compound **1** after 24 h of incubation with 1-day-old rat hepatocyte monolayer cultures and the influence of protein binding

The experiments were performed as described under *Materials and Methods*. Starting concentrations of TSA and compound **1** were 25 and 50 μ M, respectively. Peak areas obtained after HPLC-UV analysis of the samples were used to determine the relative abundances, e.g., the amount of each metabolite relative to the total amount of metabolite + parent compound (%).

Metabolite		Free	Protein Bound + Free
		%	
TSA	Trichostatic acid	9	7
	N-Didemethylated TSA amide	26	20
	Dihydro dinor trichostatic acid	0	6
	N-Monodemethylated dihydro dinor trichostatic acid	25	19
	TSA glucuronide	27	20
	Trichostatic acid glucuronide	0	3
	N-Monodemethylated TSA amide glucuronide	13	9
	N-Didemethylated TSA amide glucuronide	0	16
Compound **1**	**1**-Amide	17	12
	1-Acid	3	1
	N-Monomethylated **1**	20	8
	N-Monomethylated **1**-Acid	18	13
	1-Sulfate	1	29
	1-Glucuronide	2	1
	1-Acid sulfate	1	1
	1-Acid glucuronide	2	1
	1-Amide sulfate	6	10
	N-Monodemethylated **1**-acid sulfate	0	14
	N-Monodemethylated **1**-acid glucuronide	30	10

fold higher concentrations of the latter are needed to induce the same increase in histone acetylation in epidermal growth factor-stimulated rat hepatocyte monolayers. Furthermore, exposure to 50 μM of compound **1** arrests the cells in an earlier phase of the cell cycle than 1 μM TSA and promotes liver-specific functioning and morphology considerable more (P. Papeleu, A. Wullaert, G. Elaut, T. Henkens, M. Vinken, G. Laus, D. Tourwé, R. Beyaert, V. Rogiers, and T. Vanhaecke, submitted for publication; T. Henkens, P. Papeleu, G. Elaut, M. Vinken, V. Rogiers, and T. Vanhaecke, personal communication) (Papeleu et al., 2003).

It is not yet clear whether the inhibitors are more rapidly degraded by rat than human hepatocytes. Freshly isolated and thawed cryopreserved human hepatocytes lost approximately 50% of their membrane integrity during the 1st hour of incubation, after which viabilities remained stable, which is in line with the observations made by Blanchard et al. (2005b) and Richert et al. (2006). In contrast, the viabilities of rat hepatocytes changed only little (approximately 10%) during the entire 3-h incubation period (Elaut et al., 2005).

However, our results did show that both species more rapidly metabolize TSA than compound **1** and that similar metabolic pathways are involved. Analogous results were obtained in cryopreserved and freshly isolated human hepatocyte suspensions. As we have shown previously that one of the major phase I biotransformation pathways of TSA (i.e., HA reduction) is catalyzed by nonmicrosomal enzymes (Elaut et al., 2002), cryopreserved human hepatocyte suspensions and not human liver microsomes might be an appropriate tool for the future phase I biotransformation screening of a larger number of structurally related, potential drug candidates.

Experiments in monolayer cultures of primary adult rat hepatocytes showed that glucuronidation can be a major elimination pathway of TSA and, in particular, of compound **1**. However, the importance of this phase II detoxification pathway in vivo is as yet unknown. When TSA was administered to mice, glucuronide metabolites could not be detected in plasma (Sanderson et al., 2004). However, rodent hepatocytes can actively excrete glucuronide metabolites with a molecular mass higher than 250 Da into bile (Parkinson, 1996). Therefore, enterohepatic recirculation might play a role in the in vivo clearance of hydroxamic acid-based HDACi.

Acknowledgments

We are grateful to Prof. Daniel Jaeck and team from the Centre de Chirurgie Viscérale et de Transplantation, Hôpital de Hautepierre (Strasbourg, France) for providing the human hepatocytes. We also thank S. Coppens, B. Degreef, E. Desmedt, G. De Pauw, and H. Mertens (Department of Toxicology, Vrije Universiteit Brussel, Brussels, Belgium) for excellent technical assistance. We sincerely appreciate the contribution of Dr. P. Papeleu (Department of Toxicology, Vrije Universiteit Brussel, Brussels, Belgium) in optimizing the HDAC inhibition assay and express our thanks to Dr. G. Brosch (Department of Microbiology, University of Innsbruck, Medical School, Innsbruck, Austria) for providing the [^{3}H]acetate-prelabeled chicken reticulocyte core histones.

References

Alexandre E, Viollon-Abadie C, David P, Gandillet A, Coassolo P, Heyd B, Mantion G, Wolf P, Bachellier P, Jaeck D, et al. (2002) Cryopreservation of adult human hepatocytes obtained from resected liver biopsies. *Cryobiology* **44:**103–13.

Blanchard F and Chipoy C (2005a) Histone deacetylase inhibitors: new drugs for treatment of inflammatory diseases? *Drug Discov Today* **10:**197–204.

Blanchard N, Alexandre E, Abadie C, Lave T, Heyd B, Mantion G, Jaeck D, Richert L, and Coassolo P (2005b) Comparison of clearance predictions using primary cultures and suspensions of human hepatocytes. *Xenobiotica* **35:**1–15.

Bradford M (1976) A rapid and sensitive method for the quantitation of microgram quantities of protein utilising the principle of protein-dye binding. *Anal Biochem* **72:**248–254.

Chesné C, Guyomard C, Fautrel A, Poulain MG, Frémond B, De Jong H, and Guillouzo A (1993) Viability and function in primary culture of adult hepatocytes from various animal species and human beings after cryopreservation. *Hepatology* **18:**406–414.

Cohen LA, Amin S, Marks PA, Rikfind RA, Desai D, and Richon VM (1999) Chemoprevention of carcinogen-induced mammary tumorigenesis by the hybrid polar cytodifferentiation agent, suberanilohydroxamic acid (SAHA). *Anticancer Res* **19:** 4999–5006.

Elaut G, Török G, Vinken M, Laus G, Papeleu P, Tourwé D, and Rogiers V (2002) Major phase I biotransformation pathways of Trichostatin A in rat hepatocytes and in rat and human liver microsomes. *Drug Metab Dispos* **30:**1320–1328.

Elaut G, Török G, Papeleu P, Vanhaecke T, Laus G, Tourwé D, and Rogiers V (2004) Rat hepatocyte suspensions as a suitable in vitro model for studying the biotransformation of histone deacetylase inhibitors. *Altern Lab Anim* **32**:105–112.

Elaut G, Vanhaecke T, Vander Heyden Y, and Rogiers V (2005) Spontaneous apoptosis, necrosis, energy status, glutathione levels and biotransformation capacities of isolated rat hepatocytes in suspension: effect of the incubation medium. *Biochem Pharmacol* **69:**1829–1838.

Elaut G, Vanhaecke T, and Rogiers V (2006) The pharmaceutical potential of histone deacetylase inhibitors. Curr Pharm Design, in press.

Finnin MS, Donigian JR, Cohen A, Richon VM, Rifkind RA, Marks PA, Breslow R, and Pavletich NP (1999) Structures of a histone deacetylase homologue bound to the TSA and SAHA inhibitors. *Nature (Lond)* **401:**188–193.

Hockly E, Richon VM, Woodman B, Smith DL, Zhou X, Rosa E, Sathasivam K, Ghazi-Noori S, Mahal A, Lowden PAS, et al. (2003) Suberoylanilide hydroxamic acid, a histone deacetylase inhibitor, ameliorates motor deficits in a mouse model of Huntington's disease. *Proc Natl Acad Sci USA* **100:**2041–2046.

Jung M, Hoffman K, Brosch G, and Loidl P (1997) Analogues of trichostatin A and trapoxin B as histone deacetylase inhibitors. *Bioorg Med Chem Lett* **7:**1655–1658.

Jung M, Brosch G, Kölle D, Scherf H, Gerhäuser C, and Loidl P (1999) Amide analogues of trichostatin A as inhibitors of histone deacetylase and inducers of terminal cell differentiation. *J Med Chem* **42:**4669–4679.

Kelly WK and Marks PA (2005) Drug insight: histone deacetylase inhibitors—development of the new targeted anticancer agent suberoylanilide hydroxamic acid. *Nat Clin Pract Oncol* **2:**150–157.

Kölle D, Brosch G, Lechner T, Lusser A, and Loidl P (1998) Biochemical methods for analysis of histone deacetylases. *Methods* **15:**323–331.

Krug LM, Curley T, Schwartz L, Richardson S, Marks P, Chiao J, and Kelly WK (2006) Potential role of histone deacetylase inhibitors in mesothelioma: clinical experience with suberoylanilide hydroxamic acid. *Clin Lung Cancer* **7:**257–261.

Li AP (2001) Screening for human ADME/Tox drug properties in drug discovery. *Drug Discov Today* **6:**357–366.

Mai A, Massa A, Ragno R, Cerbara I, Jesacher F, Loidl P, and Brosch G (2003) 3-(4-Aroyl-1-methyl-1*H*-2-pyrrolyl)-*N*-hydroxy-2-alkylamides as a new class of synthetic histone deacetylase inhibitors. 1. Design, synthesis, biological evaluation, and binding mode studies performed through three different docking procedures. *J Med Chem* **46:**512–524.

Massa S, Mai A, Sbardella G, Esposito M, Ragno R, Loidl P, and Brosch G (2001) 3-(4-Aroyl-1*H*-pyrrol-2-yl)-*N*-hydroxy-2-propenamides, a new class of synthetic histone deacetylase inhibitors. *J Med Chem* **44:**2069–2072.

Niki T, Rombouts K, De Bleser P, De Smet K, Rogiers V, Schuppan D, Yoshida M, Gabbiani G, and Geerts A (1999) A histone deacetylase inhibitor, trichostatin A, suppresses myofibroblastic differentiation of rat hepatic stellate cells in primary culture. *Hepatology* **29:**858–867.

Parkinson A (1996) An overview of current cytochrome P450 technology for assessing the safety and efficacy of new materials. *Toxicol Pathol* **24:**48–57.

Papeleu P, De Smet K, Vanhaecke T, Henkens T, Elaut G, Vinken M, Snykers S, and Rogiers V (2006) Isolation of rat hepatocytes, in *Methods in Molecular Biology*, *Vol. 320, Cytochrome P450 Protocols* (Philips IR and Shephard EA eds) pp. 229–237, 2nd ed, Humana Press, Totowa, NJ.

Papeleu P, Loyer P, Vanhaecke T, Elaut G, Geerts A, Guguen-Guillouzo C, and Rogiers V (2003) Trichostatin A induces differential cell cycle arrests but does not induce apoptosis in primary cultures of mitogen-stimulated rat hepatocytes. *J Hepatol* **39:**374–382.

Piekarz R and Bates S (2004) A review of depsipeptide and other histone deacetylase inhibitors in clinical trials. *Curr Pharm Des* **10:**2289–2298.

Rahmani M, Reese E, Dai Y, Bauer C, Kramer LB, Huang M, Jove R, Dent P, and Grant S (2005) Cotreatment with suberanoylanilide hydroxamic acid and 17-allylamino 17-demethoxygeldanamycin synergistically induces apoptosis in Bcr-Abl+ cells sensitive and resistant to STI571 (imatinib mesylate) in association with down-regulation of Bcr-Abl, abrogation of signal transducer and activator of transcription 5 activity, and Bax conformational change. *Mol Pharmacol* **67:**1166–1176.

Richert L, Liguori MJ, Abadie C, Heyd B, Mantion G, Halkic N, and Waring JF (2006) Gene expression in human hepatocytes in suspension after isolation is similar to the liver of origin, is not affected by hepatocyte cold storage and cryopreservation, but is strongly changed after hepatocyte plating. *Drug Metab Dispos* **34:**870–879.

Rogiers V, Snykers S, Papeleu P, Vinken M, Henkens T, Elaut G, and Vanhaecke T (2004) Differentiation of stem cells and stabilization of phenotypical properties of primary cells. WO2006/045331. 2006 May 4.

Rombouts K, Niki T, Greenwel P, Vandermonde A, Wielant A, Hellemans K, De

Bleser P, Yoshida M, Schuppan D, Rojkind M, and Geerts A (2002) Actin filament formation, reorganization and migration are impaired in hepatic stellate cells under influence of trichostatin A, a histone deacetylase inhibitor. *Exp Cell Res* **278:**184–197.

Sanderson L, Taylor GW, Aboagye EO, Alao JP, Latigo JR, Coombes RC, and Vigushin DM (2004) Plasma pharmacokinetics and metabolism of the histone deacetylase inhibitor Trichostatin A after intraperitoneal administration to mice. *Drug Metab Dispos* **32:**1132–1138.

Snykers S, Vanhaecke T, Papeleu P, Henkens T, Vinken M, Elaut G, Van Riet I, and Rogiers V (2006) In vitro multipotency of human bone marrow (mesenchymal) stem cells. *ALTEX* **23:**400–405.

Vanhaecke T, Henkens T, Kass GEN, and Rogiers V (2004a) Effect of the histone deacetylase inhibitor Trichostatin A on spontaneous apoptosis in various types of adult rat hepatocyte cultures. *Biochem Pharmacol* **68:**753–760.

Vanhaecke T, Papeleu P, Elaut G, and Rogiers V (2004b) Trichostatin A-like hydroxamate histone deacetylase inhibitors as therapeutic agents: toxicological point of view. *Curr Med Chem* **11:**1629–1643.

Van Ommeslaeghe K, Elaut G, Brecx V, Papeleu P, Iterbeke K, Tourwé D, and Rogiers V (2003) Amide analogues of TSA: synthesis, binding mode analysis and HDAC inhibition. *Bioorg Med Chem Lett* **13:**1861–1864.

Vinken M, Henkens T, Vanhaecke T, Papeleu P, Geerts A, Chipman JK, Meda P, and Rogiers V (2006) Trichostatin A enhances gap junctional intercellular communication in primary cultures of adult rat hepatocytes. *Toxicol Sci* **91:**484–492.

Address correspondence to: Prof. Dr. Tamara Vanhaecke, Department of Toxicology, Vrije Universiteit Brussel, Laarbeeklaan 103, B-1090 Brussels, Belgium. E-mail: tamara.vanhaecke@vub.ac.be